PROCEEDINGS OF THE ROYAL SOCIETY A

Proc. R. Soc. A (2008) **464**, 2365–2390
doi:10.1098/rspa.2008.0029
Published online 25 April 2008

The unrestrainable growth of a shear band in a prestressed material

By D. Bigoni* and F. Dal Corso

Department of Mechanical and Structural Engineering, University of Trento, via Mesiano 77, 38050 Trento, Italy

A weak line inclusion model in a nonlinear elastic solid is proposed to analytically quantify and investigate, for the first time, the stress state and growth conditions of a finite-length shear band in a ductile prestressed metallic material. The deformation is shown to become highly focused and aligned coaxial to the shear band—a finding that provides justification for the experimentally observed strong tendency towards rectilinear propagation—and the energy release rate to blow up to infinity, for incremental loading occurring when the prestress approaches the elliptic boundary. It is concluded that the propagation becomes 'unrestrainable', a result substantiating the experimental observation that shear bands are the preferential near-failure deformation modes.

Keywords: failure of ductile materials; strain localization; energy release rate; slip surface growth

1. Introduction

Localized deformations in the form of shear bands emerging from a slowly varying deformation field are known to be the preferential near-failure deformation modes of ductile materials (e.g. Fenistein & van Hecke 2003; Bei *et al.* 2006; Lewandowski & Greer 2006; Rittel *et al.* 2006). Therefore, shear band formation is the key concept to explain failure in many materials and, according to its theoretical and 'practical' importance, it has been the focus of an enormous research effort in the last 30 years. From the theoretical point of view, this effort has been mainly directed in two ways,[1] namely the dissection of the specific constitutive features responsible for strain localization in different materials[2] and

* Author for correspondence (bigoni@ing.unitn.it).

Electronic supplementary material is available at http://dx.doi.org/10.1098/rspa.2008.0029 or via http://journals.royalsociety.org.

[1] Features of strain localization occurring *after* its onset have scarcely been theoretically explored. For instance, there is almost nothing about post-localization behaviour. Research devoted to this topic has been developed by Hutchinson & Tvergaard (1981), Tvergaard (1982), Petryk & Thermann (2002) and Gajo *et al.* (2004).

[2] This line of research has been initiated by Rudnicki & Rice (1975) and developed in a number of directions (including gradient effects (Aifantis 1987; Aifantis & Willis 2005), temperature effects (Gioia & Ortiz 1996; Benallal & Bigoni 2004), anisotropy effects (Bigoni & Loret 1999) and yield-vertex effects (Petryk & Thermann 2002)).

Received 24 January 2008
Accepted 12 March 2008

the struggle for the overcoming of difficulties connected with numerical approaches.[3] Although these problems still seem far from being definitely solved, the most important questions in this research area have only marginally been approached and are therefore still awaiting explanation. They are as follows.

(i) The highly inhomogeneous stress/deformation state developing near a shear band tip is unknown from an analytical point of view (and numerical techniques can hardly have the appropriate resolution to detail this).
(ii) It is not known if a shear band tip involves a strong stress concentration.
(iii) The fact that shear bands grow quasi-statically and *rectilinearly* for remarkably long distances under mode II loading conditions, while the same feature is not observed in the akin problem of crack growth, remains unexplained.
(iv) Finally, and most importantly, the reason why shear bands are preferential failure modes for quasi-statically deformed ductile materials has no justification.

Surprisingly, analytical investigation of the above problems and even of the stress field generated by a finite-length shear band, possibly including near-tip singularities, has never been attempted. Moreover, shear band growth has been considered only in a context pertaining to slope-stability problems in soil mechanics (Palmer & Rice 1973; Rice 1973), an approach recently developed by Puzrin & Germanovich (2005).

A full-field solution is given here for a finite-length shear band[4] in an anisotropic, prestressed, nonlinear elastic material, incrementally loaded under mode II and revealing: stress singularity; high inhomogeneity of the deformation and its focusing parallel and coaxially aligned to the shear band. Moreover, the incremental energy release rate is shown to blow up when the stress state approaches the condition for strain localization (i.e. the elliptic boundary). These general findings are applied to the so-called 'J_2-deformation theory material', the most important constitutive model for the plastic response of ductile metals,[5] and provide justification to the above-mentioned aspects of shear banding in ductile materials.

[3] Reviews on the numerical work developed in these years have been given by Needleman & Tvergaard (1983) and Petryk (1997).

[4] In addition to the shear band solution, we provide in appendix B the full-field solution for a finite-length crack in a prestressed material loaded incrementally under modes I and II. This solution is new in the case when the crack is inclined with respect to the material's orthotropic axes and is fundamental to the understanding of the shear band problem. Although based on the assumption that dead loading tractions are present inside the crack to equilibrate the assumed prestress state, this solution is interesting in itself, when used near the boundary of ellipticity loss, since it reveals features related to the interaction between shear bands and crack tip fields, so that it may explain experimental observations relative to crack growth in ductile materials (McClintock 1971; Hallbäck & Nilsson 1994).

[5] The finite-strain J_2-deformation theory of plasticity has been proposed by Hutchinson & Neale (1979). This theory accounts for the most important features of plastic flow in metals (except for the possibility of elastic unloading, which is *a priori* ruled out) and correctly predicts the onset of shear banding (see Hutchinson & Tvergaard 1981).

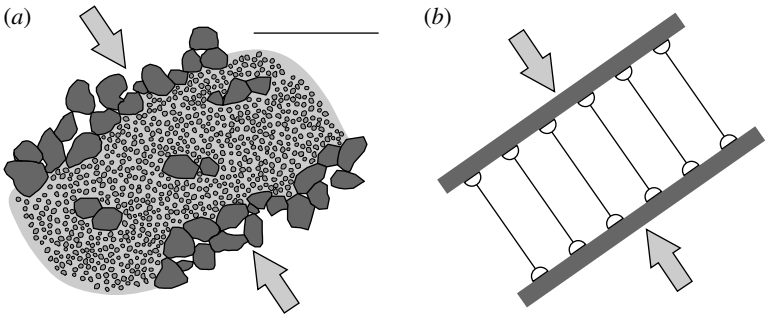

Figure 1. Sketch of (*b*) a weak interface to model (*a*) a shear band (inspired by a deformation band observed in dry sandstone by Sulem & Ouffroukh (2006)). The hinged quadrilateral should be thought to have zero thickness, so that materials in contact can freely slide incrementally along a weak surface, across which normal incremental displacement remains continuous. Scale bar, 1 mm.

2. The shear band model

A shear band of finite length, formed inside a material at a certain stage of continued deformation, is a very thin layer of material across which the normal component of incremental displacement and of nominal traction remain continuous, but the incremental nominal tangential traction vanishes, while the corresponding displacement becomes unprescribed (figure 1). Therefore, it results spontaneous to model such a shear band as a weak surface along which neighbouring materials can freely slide, but are constrained to remain in contact. Note that this slip surface is different from a crack since it can carry normal tractions, so that only under special symmetry conditions on the prestress state it may behave as a crack when subjected to shear parallel to it (the so-called 'mode II' loading in fracture mechanics).

Models of slip bands similar to the weak line model have been proposed in metal plasticity (e.g. Cottrell 1953, §10) and geomechanics (Palmer & Rice 1973; Rice 1973; Puzrin & Germanovich 2005), although the neighbouring materials assumed in these models are free of prestress and linear elastic so that there is no correlation between the shear band and the surrounding stress that has generated it.

The key to the analysis of the stress/deformation fields near a shear band and its advance under load increments is a perturbative approach similar to that proposed by Bigoni & Capuani (2002, 2005) and Piccolroaz *et al.* (2006). In particular, an infinite, incompressible, nonlinear elastic material is considered, homogeneously deformed under the plane strain condition. According to the Biot (1965) theory, the response to an incremental loading is expressed in terms of the nominal (unsymmetrical) stress increment $\dot{\boldsymbol{t}}$, related to the gradient of incremental displacement $\nabla\boldsymbol{v}$ (satisfying the incompressibility constraint tr $\nabla\boldsymbol{v}=0$) through the linear relation

$$\dot{\boldsymbol{t}} = \mathbb{K}[\nabla\boldsymbol{v}^{\mathrm{T}}] + \dot{p}\boldsymbol{I}, \tag{2.1}$$

where T denotes the transpose; $\dot{p}$ is the incremental in-plane mean stress; and the fourth-order tensor $\mathbb{K}$ is a function of the current state of stress (expressed through the principal components of Cauchy stress, σ_1 and σ_2) and material

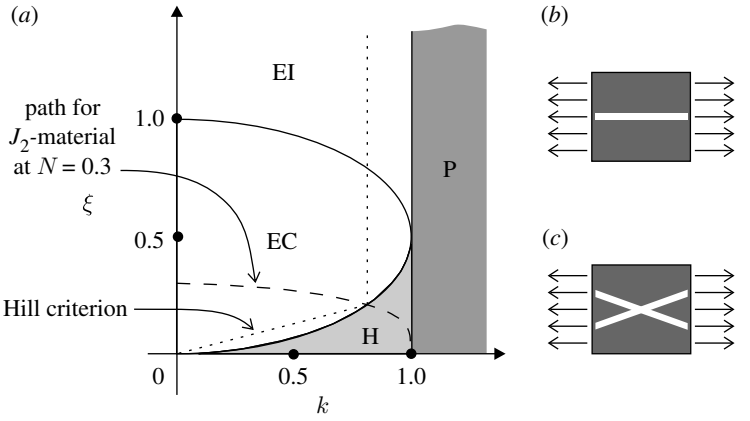

Figure 2. (*a*) Regime classification as a function of the orthotropy ratio ξ versus the prestress parameter k, taken as positive. Shear bands (planes across which the incremental displacement gradient is discontinuous) aligned parallel to the principal tensile stress direction emerge at (*b*) the EI/P boundary, while inclined shear bands become possible at (*c*) the EC/H boundary. The path leading to the EC/H boundary and corresponding to the continued deformation of a ductile low-hardening metal (modelled as a J_2-deformation theory material with hardening exponent N=0.3) is shown as dashed curve and occurs for a proper choice of the parameter η, when the Hill exclusion condition (whose right boundary is shown as dotted line) holds (appendix A).

response to shear (μ for shear parallel and μ_* for shear inclined at $\pi/4$ with respect to σ_1) describing orthotropy (aligned parallel to the current principal stress directions; see appendix A for details). All parameters defining $\mathbb{K}$ and representing the current state of the material can be condensed into the following dimensionless quantities:

$$\xi = \frac{\mu_*}{\mu}, \qquad \eta = \frac{\sigma_1 + \sigma_2}{2\mu}, \qquad k = \frac{\sigma_1 - \sigma_2}{2\mu}, \tag{2.2}$$

where μ and μ_* may be arbitrary functions of the current stress and/or strain.

The differential equations governing incremental equilibrium can be classified according to the values assumed by parameters ξ and k, to distinguish between elliptic imaginary (EI), elliptic complex (EC), parabolic (P) and hyperbolic (H) regimes (figure 2*a*).

According to the conventional approach (Biot 1965; Rudnicki & Rice 1975), shear bands are understood as planes across which incremental velocity gradient becomes discontinuous and may emerge only in a continuous deformation path as soon as either the EC/H or EI/P boundary is 'touched'. Two equally inclined (with respect to the principal stress directions) bands are generated in the former case (figure 2*c*), while only one band forms aligned with the principal maximum tensile stress, say σ_1, in the latter case (figure 2*b*). Following the alternative approach (Bigoni & Capuani 2002, 2005; Piccolroaz *et al.* 2006), shear bands spontaneously emerge as the response to a perturbation applied inside the elliptic regime, but in the vicinity of either the EI/P or EC/H boundary. Since experiments suggest that shear banding is strongly influenced by the presence of

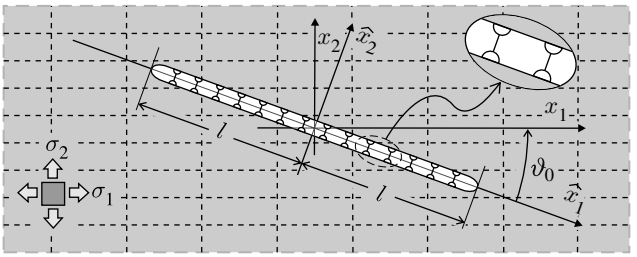

Figure 3. Finite-length ($2l$) shear band in a prestressed orthotropic material inclined at an angle ϑ_0 (positive when anticlockwise) with respect to the orthotropy axes x_1 and x_2. The prestress state is expressed through the two in-plane principal Cauchy stresses σ_1 and σ_2, aligned parallel to the x_1–x_2 reference system. The null shear stiffness at the band boundaries has to be understood in an incremental sense.

randomly distributed defects (Xue & Gray 2006), it is assumed that during homogeneous deformation of an infinite medium subjected to remote stress with $k>0$, a defect is present in the form of a thin zone of material that has touched the EI/P or EC/H boundary and has been transformed into a shear band of length $2l$ (in other words, the weak line inclusion in the proposed modelling), leaving the surrounding material uniformly deformed/stressed and still in the elliptic regime, although near the elliptic boundary. (This uniform state of stress has to satisfy the Hill exclusion condition, to avoid 'spurious' interfacial instabilities; see appendix A.) The shear band of length $2l$ is inclined with respect to the x_1-axis at an angle ϑ_0 that can be determined from a known formula (Hutchinson & Tvergaard 1981), thus providing the inclination of the weak line inclusion with respect to the material orthotropy x_1-axis (figure 3). Taking this configuration as the initial state, the response of the shear band to an incremental perturbation is analysed.

According to the weak line model, under an incremental mode I perturbation the shear band does not alter the incremental response of the surrounding material (so that it is 'neutral'), but under a mode II perturbation the shear band behaves as a slip surface of length $2l$ (prestressed both longitudinally and transversely), and strongly non-uniform and singular fields are generated.

3. Analytical solution for a shear band of finite length loaded incrementally

The analytical solution for a finite-length crack incrementally loaded by a uniform mode II far field in a prestressed material similar to that described by equation (2.1) was available only when the crack is aligned parallel or orthogonal to the orthotropy axes, a situation corresponding to a shear band forming at the EI/P boundary, where symmetry implies that a crack behaves as a slip surface, so that the crack and the weak line become equivalent models. The solution for an inclined crack in a prestressed material (obtained in appendix B) is interesting in itself (since it shows features of interactions between shear bands and crack tip fields) and of fundamental importance for the understanding of the shear band problem addressed here.

For shear bands occurring at the EC/H boundary, the solution for a weak line inclusion inclined with respect to the orthotropy axes, not previously available for the material under consideration, is given here. Developing this solution for constitutive equations (2.1) and employing it to analyse a shear band, a $1/\sqrt{r}$ singularity is found. Moreover, *a full-field representation is obtained for the incremental stress/strain field near a shear band of finite length.*

The solution for an inclined shear band in an infinite medium can be expressed in a $\hat{x}_1$–$\hat{x}_2$ reference system located at the shear band centre, with the $\hat{x}_1$-axis aligned parallel to the shear band, and rotated at an angle ϑ_0 with respect to the reference system in which constitutive equations (2.1) are expressed (figure 3).

The stress components in the $\hat{x}_1$–$\hat{x}_2$ reference system can be obtained through a rotation of the components in the prestress principal reference system x_1–x_2, so that, since the two systems are rotated at an angle ϑ_0 (taken positive when anticlockwise), we have

$$\hat{\boldsymbol{x}} = \boldsymbol{Q}^{\mathrm{T}}\boldsymbol{x}, \quad [\boldsymbol{Q}] = \begin{bmatrix} \cos\vartheta_0 & \sin\vartheta_0 \\ -\sin\vartheta_0 & \cos\vartheta_0 \end{bmatrix}, \tag{3.1}$$

so that the nominal stress increment, incremental displacement and its gradient can be expressed in the $\hat{x}_1$–$\hat{x}_2$ reference system as

$$\hat{\boldsymbol{t}} = \boldsymbol{Q}^{\mathrm{T}}\boldsymbol{t}\,\boldsymbol{Q}, \qquad \hat{\boldsymbol{v}} = \boldsymbol{Q}^{\mathrm{T}}\boldsymbol{v}, \qquad \hat{\nabla}\hat{\boldsymbol{v}} = \boldsymbol{Q}^{\mathrm{T}}\nabla\boldsymbol{v}\boldsymbol{Q}, \tag{3.2}$$

while the constitutive equations (2.1) transform to

$$\hat{\boldsymbol{t}} = \hat{\mathbb{K}}[\hat{\nabla}\hat{\boldsymbol{v}}^{\mathrm{T}}] + \dot{p}\boldsymbol{I}, \tag{3.3}$$

where the transformed fourth-order tensor $\hat{\mathbb{K}}$ is given by

$$\hat{\mathbb{K}}_{ijhk} = Q_{li}Q_{mj}\mathbb{K}_{lmno}Q_{nh}Q_{ok}, \tag{3.4}$$

where the indices range between 1 and 2.

In the $\hat{x}_1$–$\hat{x}_2$ reference system, the so-called 'perturbed problem' is solved in which the traction at infinity $\hat{t}^{\infty}_{21}$ is applied with reversed sign along the shear band surfaces. In terms of perturbed stream function $\hat{\psi}^{\circ}$, defined to provide the incremental displacements as

$$\hat{v}^{\circ}_1 = \frac{\partial\hat{\psi}^{\circ}}{\partial\hat{x}_2}, \qquad \hat{v}^{\circ}_2 = -\frac{\partial\hat{\psi}^{\circ}}{\partial\hat{x}_1}, \tag{3.5}$$

the full-field solution for a shear band of length $2l$ can be written as

$$\hat{\psi}^{\circ}(\hat{x}_1,\hat{x}_2) = \frac{\hat{t}^{\infty}_{21}}{2\mu}\sum_{j=1}^{2}\mathrm{Re}\big[B^{\mathrm{II}}_j f(\hat{z}_j)\big], \tag{3.6}$$

where

$$f(\hat{z}_j) = \hat{z}_j^2 - \hat{z}_j\sqrt{\hat{z}_j^2 - l^2} + l^2\ln\left(\hat{z}_j + \sqrt{\hat{z}_j^2 - l^2}\right) \tag{3.7}$$

and (Ω_j is purely imaginary in EI and complex in EC and Re denotes the real part of its argument)

$$\left.\begin{aligned} \hat{z}_j &= \hat{x}_1 + W_j \hat{x}_2, \qquad & W_j &= \frac{\sin\vartheta_0 + \Omega_j \cos\vartheta_0}{\cos\vartheta_0 - \Omega_j \sin\vartheta_0}, \\ \Omega_j^2 &= \frac{1-2\xi + (-1)^j \Lambda}{1-k}, \qquad & \Lambda &= \sqrt{4\xi^2 - 4\xi + k^2}. \end{aligned}\right\} \tag{3.8}$$

The unknown complex constants B_j^{II} ($j=1, 2$) in equation (3.6) can be determined by imposing boundary conditions at the shear band surfaces, namely

— null incremental nominal shearing tractions

$$\hat{t}_{21}(\hat{x}_1, 0^{\pm}) = 0, \quad \forall\, |\hat{x}_1| < l; \tag{3.9}$$

— continuity of the incremental nominal normal traction

$$[\![\hat{t}_{22}(\hat{x}_1, 0)]\!] = 0, \quad \forall\, |\hat{x}_1| < l; \tag{3.10}$$

— continuity of normal incremental displacement

$$[\![\hat{v}_2(\hat{x}_1, 0)]\!] = 0, \quad \forall\, |\hat{x}_1| < l; \tag{3.11}$$

where the brackets $[\![\cdot]\!]$ denote the jump of the relevant argument across the shear band.

Employing equation (3.6) and imposing the boundary conditions (3.9)–(3.11) at the sliding surface yields the following algebraic system for the unknown constants B_j^{II}:

$$\begin{bmatrix} -c_{21} & c_{11} & -c_{22} & c_{12} \\ c_{31} & c_{41} & c_{32} & c_{42} \\ -c_{41} & c_{31} & -c_{42} & c_{32} \\ 0 & 1 & 0 & 1 \end{bmatrix} \begin{bmatrix} \mathrm{Re}\,[B_1^{\mathrm{II}}] \\ \mathrm{Im}\,[B_1^{\mathrm{II}}] \\ \mathrm{Re}\,[B_2^{\mathrm{II}}] \\ \mathrm{Im}\,[B_2^{\mathrm{II}}] \end{bmatrix} = \begin{bmatrix} 0 \\ -1 \\ 0 \\ 0 \end{bmatrix}, \tag{3.12}$$

where coefficients c_{ij} are defined by equations (B 6). The determinant of the coefficient matrix in equation (3.12) vanishes both when the surface bifurcation condition, equation (A 18), is met and at the EC/H boundary.

Similar to the crack solution, the asymptotic fields near the shear band tip result to be given in polar coordinates (centred at the shear band tip ($\hat{x}_1 = l,\ \hat{x}_2 = 0$)) by

$$\hat{t}_{22}(r, 0) = -\frac{\Upsilon \dot{K}_{\mathrm{II}}}{\sqrt{2\pi r}}, \qquad \hat{t}_{21}(r, 0) = \frac{\dot{K}_{\mathrm{II}}}{\sqrt{2\pi r}}, \tag{3.13}$$

for the incremental nominal stress ahead of the tip, where

$$\Upsilon = \frac{\hat{t}_{22}^{\circ}}{\hat{t}_{21}^{\infty}} = c_{11}\,\mathrm{Re}\,[B_1^{\mathrm{II}}] + c_{12}\,\mathrm{Im}\,[B_1^{\mathrm{II}}] + c_{13}\,\mathrm{Re}\,[B_2^{\mathrm{II}}] + c_{14}\,\mathrm{Im}\,[B_2^{\mathrm{II}}], \tag{3.14}$$

while for the incremental displacements we have (where constants have been neglected)

$$\left.\begin{aligned}\hat{v}_1(\Delta l - r,\ \pm\pi) &= \pm\frac{\hat{t}_{21}^{\infty}\sqrt{2l}\sqrt{\Delta l - r}}{2\mu}\ \mathrm{Im}\left[W_1 B_1^{\mathrm{II}} + W_2 B_2^{\mathrm{II}}\right],\\ \hat{v}_2(\Delta l - r,\ \pm\pi) &= \mp\frac{\hat{t}_{21}^{\infty}\sqrt{2l}\sqrt{\Delta l - r}}{2\mu}\ \mathrm{Im}\left[B_1^{\mathrm{II}} + B_2^{\mathrm{II}}\right],\end{aligned}\right\} \tag{3.15}$$

holding at the shear band surfaces, for 'small' Δl.[6]

In the particular case of a shear band aligned parallel to the prestress principal direction σ_1 (i.e. $\vartheta_0 = 0$), solution (3.6) simplifies to

$$\hat{\psi}^{\circ} = -\frac{\hat{t}_{21}^{\infty}}{2\mu}\ \mathrm{Re}\left[\frac{\sum_{j=1}^{2}(-1)^j(2\xi - \eta - (-1)^j\Lambda)\sqrt{2\xi - 1 + (-1)^j\Lambda}f(\hat{z}_j)}{(2\xi-\eta+\Lambda)^2\sqrt{2\xi-1-\Lambda} - (2\xi-\eta-\Lambda)^2\sqrt{2\xi-1+\Lambda}}\right]. \tag{3.16}$$

4. Rectilinear shear band growth is a preferred failure mode

Solution (3.6) is employed to obtain results shown in figure 4, where level sets of incremental deviatoric strain are reported for a shear band (inclined at 29.3°) in a ductile low-hardening metal, modelled through the J_2-deformation theory with $N = 0.3$, at null prestrain $\varepsilon = 0$ (figure 4*a*) and at a prestrain $\varepsilon = 0.548$ (figure 4*b*), taken close to the EC/H boundary. It can be noted from the figure (additional results are reported in appendix C) that, while at null prestrain (far from the elliptic boundary in figure 4*a*) the incremental strain field is not particularly developed and does not evidence focusing, near the elliptic boundary (figure 4*b*) *the incremental strain field is localized and elongated, and evidences a strong focusing in the direction aligned parallel to the shear band*. This finding suggests that, *while mode II rectilinear crack propagation in a homogeneous material does not usually occur* (*since in first approximation cracks deviate from rectilinearity following the maximum near-tip hoop stress inclination*), *shear band growth is very likely to occur aligned with the shear band itself*. This observation explains the strong tendency that shear bands evidence towards the rectilinear propagation for long (compared with their thickness) distances (e.g. Korbel & Bochniak 2004; Bei *et al.* 2006). Moreover, the focusing of incremental deformation and the stress singularity strongly promotes shear band growth.

[6] The following properties of function Υ

$$\Upsilon(k = 0, \vartheta_0) = \Upsilon(k, \vartheta_0 = 0) = \Upsilon(k, \vartheta_0 = \pi/2) = 0$$

have been proven, while the properties

$$\Upsilon = \Upsilon(k, \vartheta_0) = -\Upsilon(-k, \pi/2 - \vartheta_0)$$

have been numerically found to hold, from which the identities

$$\Upsilon(k, \vartheta_0 = \pi/4) = \frac{1 - \sqrt{1-k^2}}{k} \quad \text{and} \quad \Upsilon(k, \vartheta_0 = \pi/3) = \frac{\sqrt{3}(2 + k - 2\sqrt{1-k^2})}{4 + 5k}$$

follow with the help of a symbolic manipulator.

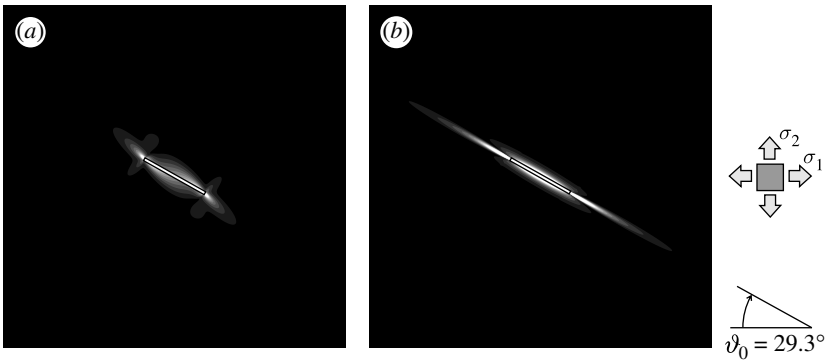

Figure 4. Level sets of the modulus of incremental deviatoric strain, near a shear band of length $2l$ (demonstrated by a thin rectangle, providing the scale bar of the representation) in a low-hardening ductile metal (a J_2-deformation theory material with $N=0.3$). (*a*) Null prestrain, $\varepsilon=0$, and (*b*) uniform prestrain near the EH/C boundary, $\varepsilon=0.548$, are considered for mode II incremental loading parallel to the shear band (inclined at $\vartheta_0=29.3°$ with respect to the principal Cauchy stress direction σ_1). Parameter η has been taken as equal to $0.52k$, so that the Hill exclusion condition holds.

To further analyse shear band growth, *the incremental energy release rate for an infinitesimal shear band advance* (see appendix B*c*) can be calculated for an orthotropic prestressed material, equation (2.1), by employing the asymptotic near-tip representations (3.13) and (3.15) in equation (B 19)[7]

$$\dot{G}^{\mathrm{sb}} = \dot{K}_{\mathrm{II}}^2 \frac{\mathrm{Im}\left[W_1 B_1^{\mathrm{II}} + W_2 B_2^{\mathrm{II}}\right]}{4\mu}, \tag{4.1}$$

where the complex constants B_j^{II} are the solutions of equation (3.12). Equation (4.1) becomes, for a shear band aligned parallel to the principal direction of prestress σ_1 ($\vartheta_0=0$),

$$\dot{G}^{\mathrm{sb}} = \frac{\dot{K}_{\mathrm{II}}^2}{\mu} \frac{\Lambda\sqrt{1+k}}{(2\xi-\eta+\Lambda)^2\sqrt{2\xi-1-\Lambda}-(2\xi-\eta-\Lambda)^2\sqrt{2\xi-1+\Lambda}}. \tag{4.2}$$

[7] Note that the perturbed solution for the shear band model can be alternatively obtained providing a mixed-mode loading to an inclined crack (see appendix B*a*). The mode I loading component is 'calibrated' with respect to the mode II component in such a way as to eliminate the jump in normal incremental displacement along the crack faces generated by a pure mode II loading, in other words, to satisfy condition (3.11). All these procedures bear on the special feature found in the solution of the crack problem that a mode I uniform loading along the crack faces is sufficient to eliminate a mode II transversal mismatch in incremental displacements. In particular equation (4.1) can be obtained from equation (B 23), considering a mixed mode defined by $\hat{t}_{22}^{\infty}=-\Upsilon\hat{t}_{21}^{\infty}$, so that the condition of continuity of transversal incremental displacement yields

$$\mathrm{Im}\,[A_1^{\mathrm{II}} + A_2^{\mathrm{II}}] - \Upsilon\,\mathrm{Im}\,[A_1^{\mathrm{I}} + A_2^{\mathrm{I}}] = 0,$$

and the constants defining the crack and shear band solutions are related through

$$B_j^{\mathrm{II}} = A_j^{\mathrm{II}} - \Upsilon A_j^{\mathrm{I}}, \quad j=1,2.$$

Therefore, the difference between the crack and shear band problems lies in a uniform nominal normal stress increment applied at the crack surfaces.

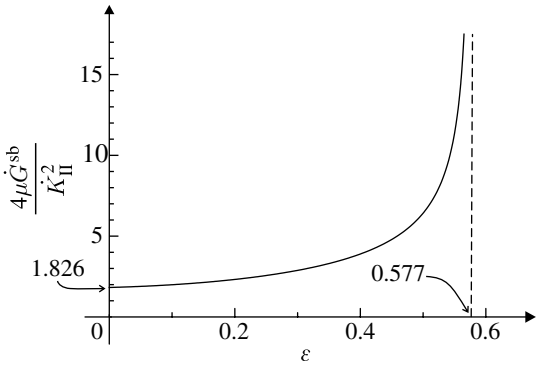

Figure 5. Incremental energy release rate $\dot{G}^{sb}$ (made dimensionless by multiplying by $4\mu/\dot{K}_{II}^2$) for an infinitesimal growth of a shear band (inclined at $\vartheta_0 = 29.3°$) in a low-hardening ductile metal (a J_2-deformation theory material with $N = 0.3$ and $\eta = 0.52k$), as a function of the prestrain parameter ε, equal to 0.577 at the EC/H boundary, so that shear band growth becomes 'unrestrainable' when this boundary is approached.

In equations (4.1) and (4.2) constant $\dot{K}_{II}$ is the incremental mode II stress intensity factor, defining the intensity of the singularity in terms of applied incremental loading $\hat{t}_{21}^{\infty}$ and equal to

$$\dot{K}_{II} = \hat{t}_{21}^{\infty}\sqrt{\pi l}, \tag{4.3}$$

for a rectilinear shear band of length $2l$ in an infinite material (inclined with respect to the orthotropy and prestress axes).

The release rate (4.1) represents the energy released for an infinitesimal advance of the shear band and has the typical behaviour shown in figure 5, referred to the same material considered in figure 4 (there are no qualitative changes when other values of the hardening exponent N are considered, see appendix C).

It is assumed in fracture mechanics that a crack advances under small-scale yielding when the energy release rate exceeds a critical threshold, believed to be a characteristic of the material. Whether this criterion can be generalized to the present context or not can still be a matter of discussion, but the important point is that *the incremental energy release rate blows up to infinity when the elliptic boundary is approached*. In these conditions, a shear band can drive itself on and overcome possible barriers; in other words, it can grow 'unrestrainable', a finding which, together with the previous results on near-tip stress/deformation states, legitimizes for the first time the common experimental observation that shear bands are the preferred near-failure deformation modes.

5. Conclusions

The modelling of a finite-length shear band in an infinite prestressed material presented in this article keeps into account stress-induced and inherent anisotropy, and large strain effects. Quasi-statically loaded ductile materials have been addressed exhibiting incompressible flow, typically metals, and the modelling permits the first explicit closed-form evaluation of all mechanical fields near a shear band of finite length and provides justification to the fact that shear bands are preferred modes growing rectilinearly for long distances, as experimentally found by

Korbel & Bochniak (2004) among others. A number of features in the modelling of the material (the possibility of elastic unloading outside the shear band, dynamic loading and thermal effects and, for granular materials and soils, pressure sensitivity of yielding and plastic flow dilatancy) and of the shear band (the possibility of introducing cohesive tangential forces between the weak line surfaces) have been sacrificed for mathematical tractability, although their incorporation can certainly be pursued. In particular, elastic unloading near the shear band and thermal effects have been found to be important (the latter when dynamic loading is involved, Guduru *et al.* (2001), while the former even for quasi-static loading, Gajo *et al.* (2004)) and the development of weak cohesive forces at the shear band surfaces might prelude the extreme loss of (incremental) stiffness assumed in our model. However, considering our previous treatment of various perturbations in materials prestressed near the boundary of ellipticity loss (Bigoni & Capuani 2002, 2005; Piccolroaz *et al.* 2006), we believe that the results presented in this article have general validity and can be extended to include much more complicated effects.

Financial support of Trento University is gratefully acknowledged.

Appendix A. Incremental constitutive equations for incompressible nonlinear elasticity

According to the Biot (1965) theory, the response of a nonlinear elastic, incompressible and uniformly deformed material subjected to an incremental loading is expressed in terms of the nominal (unsymmetrical) stress increment $\dot{\boldsymbol{t}}$, related to the gradient of incremental displacement $\nabla\boldsymbol{v}$ (satisfying the incompressibility constraint $\operatorname{tr}\nabla\boldsymbol{v}=0$) through the linear relation (2.1) where the components of constitutive fourth-order tensor $\mathbb{K}$ (possessing the major symmetry $\mathbb{K}_{ijhk}=\mathbb{K}_{hkij}$) are

$$\left.\begin{array}{lll} \mathbb{K}_{1111}=\mu(\xi-k-\eta), & \mathbb{K}_{1122}=-\mu\xi, & \mathbb{K}_{1112}=\mathbb{K}_{1121}=0, \\ \mathbb{K}_{2211}=-\mu\xi, & \mathbb{K}_{2222}=\mu(\xi+k-\eta), & \mathbb{K}_{2212}=\mathbb{K}_{2221}=0, \\ \mathbb{K}_{1212}=\mu(1+k), & \mathbb{K}_{1221}=\mathbb{K}_{2112}=\mu(1-\eta), & \mathbb{K}_{2121}=\mu(1-k). \end{array}\right\} \quad \text{(A 1)}$$

The components of the constitutive fourth-order tensor $\mathbb{K}$ depend on the current state of stress (expressed through the principal components of Cauchy stress, σ_1 and σ_2) and material response to shear (μ for shear parallel and μ_* for shear inclined at $\pi/4$ with respect to σ_1) describing orthotropy (aligned parallel to the current principal stress directions), see Bigoni & Capuani (2002, 2005) for details, through the dimensionless quantities (2.2).

(*a*) *Positive definiteness of* $\mathbb{K}$

The Hill exclusion condition for bifurcation (Hill 1958) is the condition of positive definiteness of the constitutive fourth-order tensor $\mathbb{K}$ (Hill & Hutchinson 1975, eqn (3.9)). Assuming $\mu>0$, in terms of dimensionless constants (2.2), this condition becomes

$$0<\eta<2\xi, \quad \frac{k^2+\eta^2}{2\eta}<1, \quad \text{(A 2)}$$

defining a region in the space ξ, k and η, which bound has been reported in figure 2 for $\eta/k=0.52$, see also the electronic supplementary material.

(*b*) *Regime classification*

Since the material response described by equations (2.1) and (2.2) is incompressible, we can introduce a *stream function* $\psi(x_1, x_2)$, with the property (where a comma means differentiation with respect to the corresponding spatial variable)

$$v_1 = \psi_{,2}, \qquad v_2 = -\psi_{,1}, \tag{A 3}$$

so that the incompressibility constraint is automatically satisfied. Assuming zero body forces, the elimination of $\dot{p}$ in the incremental equilibrium equations ($\dot{t}_{ij,i} = 0$) gives the fourth-order partial differential equation

$$(1+k)\psi_{,1111} + 2(2\xi - 1)\psi_{,1122} + (1-k)\psi_{,2222} = 0, \tag{A 4}$$

derived by Biot (1965, p. 193, eqn (3.7), see also Hill & Hutchinson 1975, eqn (3.3)).

Following Lekhnitskii (1981), Guz (1999), Radi *et al.* (2002), Cristescu *et al.* (2004) and Dal Corso *et al.* (2008), a solution of (A 4) can be represented in terms of the analytic function F

$$\psi(x_1, x_2) = F(x_1 + \Omega x_2), \tag{A 5}$$

where Ω is a complex constant satisfying the biquadratic equation obtained inserting representation (A 5) in equation (A 4),

$$1 + k + 2(2\xi - 1)\Omega^2 + (1-k)\Omega^4 = 0. \tag{A 6}$$

The four roots Ω_j (j=1, …, 4) of equation (A 6) satisfy equation $(3.8)_3$ and are real or complex depending on the values of ξ and k. In compact form, we write

$$\Omega_j = \alpha_j + \mathrm{i}\beta_j, \quad j = 1, \ldots, 4, \tag{A 7}$$

and define the four complex variables

$$z_j = x_1 + \Omega_j x_2 = x_1 + \alpha_j x_2 + \mathrm{i}\beta_j x_2, \qquad j = 1, \ldots, 4, \tag{A 8}$$

where $\mathrm{i} = \sqrt{-1}$ is the imaginary unit, $\alpha_j = \mathrm{Re}\,[\Omega_j]$ and $\beta_j = \mathrm{Im}\,[\Omega_j]$.

Employing equations (A 5) and (A 8), *the general solution of the differential equation* (A 4) can be written as

$$\psi(x_1, x_2) = \sum_{j=1}^{4} F_j(z_j). \tag{A 9}$$

The roots Ω_j, defined by equation $(3.8)_3$ change their nature according to the values of parameters ξ and k, so that the differential equation (A 4) can be classified as reported by Dal Corso *et al.* (2008). The regime classification in the k–ξ plane has been given by Radi *et al.* (2002) and is sketched in figure 2.

In the EI regime, defined as

$$k^2 < 1 \quad \text{and} \quad 2\xi > 1 + \sqrt{1-k^2}, \tag{A 10}$$

we have four imaginary conjugate roots Ω_j, so that

$$\alpha_1 = \alpha_2 = 0, \qquad \left.\begin{matrix}\beta_1 \\ \beta_2\end{matrix}\right\} = \sqrt{\frac{2\xi - 1 \pm \sqrt{4\xi^2 - 4\xi + k^2}}{1-k}} > 0, \tag{A 11}$$

while in the EC regime, defined as

$$k^2<1 \quad \text{and} \quad 1-\sqrt{1-k^2}<2\xi<1+\sqrt{1-k^2}, \tag{A 12}$$

we have four complex conjugate roots Ω_j, so that

$$\left.\begin{aligned}\beta&=\beta_1=\beta_2\\ \alpha&=-\alpha_1=\alpha_2\end{aligned}\right\}=\sqrt{\frac{\sqrt{1-k^2}\pm(2\xi-1)}{2(1-k)}}>0. \tag{A 13}$$

(*c*) *Specific cases of material behaviour*

The assumption of a specific material model determines the relation between ξ and k. For instance, a Mooney–Rivlin material coincides with a neo-Hookean material for plane isochoric deformations, so that parameters k and ξ become (where λ is the logarithmic stretch, representing a prestrain measure)

$$k=\frac{\lambda^2-\lambda^{-2}}{\lambda^2+\lambda^{-2}}, \quad \xi=1, \tag{A 14}$$

while for a J_2-deformation theory material (Hutchinson & Neale 1979), particularly suited to analyse the plastic branch of the constitutive response of ductile metals, we have

$$k=\frac{\lambda^4-1}{\lambda^4+1}, \qquad \xi=\frac{N(\lambda^4-1)}{2(\ln\lambda)(\lambda^4+1)}, \tag{A 15}$$

where N is the hardening exponent. The curve in the ξ versus k plane described by equation (A 15) for $N=0.3$ is reported in figure 2.

(*d*) *Shear bands inclination*

At the EC/H boundary, *two* shear bands become simultaneously possible, their inclinations are given by the angles $\pm\vartheta_0$ between the shear band and the x_1-axis and solutions of (Hill & Hutchinson 1975)

$$\cot^2\vartheta_0=\frac{1+2\,\mathrm{sign}(k)\sqrt{\xi(1-\xi)}}{1-2\xi}. \tag{A 16}$$

At the EI/P boundary, we have only *one* shear band possible, aligned parallel to the x_1-axis (x_2-axis), when $k=1$ ($k=-1$)

$$\vartheta_0=0, \quad \text{for } k=1, \quad \text{or} \quad \vartheta_0=\frac{\pi}{2}, \quad \text{for} \quad k=-1. \tag{A 17}$$

(*e*) *Surface bifurcation*

Surface instability occurs (Needleman & Ortiz 1991, eqn (48)) when

$$4\xi-2\eta=\frac{\eta^2-2\eta+k^2}{\sqrt{1-k^2}}, \tag{A 18}$$

which, in the particular case of stress parallel to the free surface $x_1=0$ ($\eta=k$), becomes

$$\xi=\frac{k}{2}\left(1-\sqrt{\frac{1-k}{1+k}}\right). \tag{A 19}$$

Surface bifurcation, equation (A 18), and the Hill exclusion condition, equation (A 2), are reported in figure 2 for $\eta/k=0.52$.

In our model of a shear band, a sliding surface abruptly (but affecting only incremental fields) forms when the thin layer of material representing the shear band touches the elliptic boundary, while in a refined model a weak thin layer of material should approach the elliptic boundary becoming incrementally less stiff in a continuous way. The abrupt formation of a sliding surface within an infinite solid may, depending on the stress conditions, generate a sudden 'spurious' interfacial instability, so that in this condition our shear band model becomes oversimplified. Therefore, the model has to be employed only in situations where surface instabilities are *a priori* excluded until the elliptic boundary is met, a circumstance that can be attained employing the Hill (1958) exclusion condition (see also Hill & Hutchinson (1975), eqn (3.9)). However, this condition is so general that all points of the EC/H and EI/P boundaries can be explored, by taking $k>0$ and selecting appropriate values for the prestress parameter η, as can be noted from figure 2, see also the electronic supplementary material.

Appendix B. Finite-length crack in a prestressed material

A homogenously prestressed and prestrained, incompressible elastic infinite plane is considered, characterized by the constitutive equations (2.1) of incremental, incompressible orthotropic elasticity, containing a crack of current length $2l$, taken parallel to the $\hat{x}_1$-axis in the $\hat{x}_1$–$\hat{x}_2$ reference system, and loaded at infinity by a uniform nominal stress increment $\hat{t}^{\infty}_{2n}$, where $n=1$ corresponds to mode II and $n=2$ to mode I loading (see figure 3, in which the shear band should be thought to represent a crack of length $2l$).

Obviously, the crack faces cannot be free of tractions, since a dead loading is required to 'provide' the prestress state (with principal Cauchy components σ_1 and σ_2, assumed to be aligned parallel to the x_1–x_2 reference system, rotated at an angle ϑ_0 with respect to the $\hat{x}_1$–$\hat{x}_2$ system). An interesting exception to this rule occurs when the crack is aligned parallel to the x_1-axis and the prestress is aligned parallel to the crack surfaces, namely when the $\hat{x}_1$–$\hat{x}_2$ and x_1–x_2 systems coincide, i.e. $\vartheta_0=0$, and $\sigma_2=0$, corresponding to $\eta=k$. This situation has been considered by Guz (1999, and references therein), Radi *et al.* (2002) (in the near-tip asymptotic limit) and Cristescu *et al.* (2004). The case of a generic inclination ϑ_0 has never been treated in the case of a prestressed material, but it is well known in linear, infinitesimal, anisotropic elasticity (Savin 1961; Sih & Liebowitz 1968).

Solution to the above-formulated crack problem is obtained by superimposing the trivial unperturbed solution to the perturbation induced by the crack, the latter denoted with the apex °.

The unperturbed solutions are obtained defining the uniform nominal stress field in the $\hat{x}_1$–$\hat{x}_2$ reference system

$$\hat{t}_{22} = \hat{t}^{\infty}_{22}, \qquad \hat{t}_{11} = 0, \qquad \hat{t}_{12} = \hat{t}_{21} = \hat{t}^{\infty}_{21}, \tag{B 1}$$

so that $\hat{t}^{\infty}_{21} = 0$ $\left(\hat{t}^{\infty}_{22} = 0\right)$ for mode I (mode II).

The nominal stress increment, incremental displacement and its gradient are expressed in the $\hat{x}_1$–$\hat{x}_2$ reference system through equations (3.1)–(3.4).

Note that the above definition (B 1) of mode I and II loading is fully meaningful only when the constitutive equations (2.1) are positive defined, so that the Hill exclusion condition (A 2) holds true. For a non-positive definite constitutive equation, definition (B 1) would be better changed to one concerning the components of the incremental displacement gradient.

Assuming that condition (A 2) holds true, we can directly obtain from equations (2.1), (2.2) and (A 1) the components of the incremental displacement gradient and the incremental in-plane mean stress in the x_1–x_2 reference system

$$\left.\begin{aligned} \dot{p} &= \frac{\hat{t}^{\infty}_{22}}{2} - \mu k v_{2,2}, \\ v_{2,2} &= -v_{1,1} = \frac{\hat{t}^{\infty}_{22}\cos 2\vartheta_0 - 2\hat{t}^{\infty}_{21}\sin 2\vartheta_0}{2\mu(2\xi - \eta)}, \\ v_{1,2} &= -\frac{(k+\eta)\left(\hat{t}^{\infty}_{22}\sin 2\vartheta_0 + 2\hat{t}^{\infty}_{21}\cos 2\vartheta_0\right)}{2\mu(k^2 - 2\eta + \eta^2)}, \\ v_{2,1} &= \frac{(k-\eta)\left(\hat{t}^{\infty}_{22}\sin 2\vartheta_0 + 2\hat{t}^{\infty}_{21}\cos 2\vartheta_0\right)}{2\mu(k^2 - 2\eta + \eta^2)}. \end{aligned}\right\} \tag{B 2}$$

The components of the incremental displacement gradient in the $\hat{x}_1$–$\hat{x}_2$ reference system can be obtained through a rotation of equations (B 2), by employing equation $(3.2)_3$.

It should be noted from equations (B 2) that in the absence of prestress, $k = \eta = 0$, equations (B 2) fully determine the incremental displacement gradient. However, in this case, the incremental stress is only related to the symmetric part of the incremental displacement gradient, so that an arbitrary incremental rotation can be added without altering the state of stress, a circumstance not possible when the prestress is different from zero. In other words, when the prestress is present, loading (B 1) completely defines the incremental displacement gradient (and incremental mean stress) through equations (B 2), so that the incremental rigid-body rotations remain determined.

(*a*) *The inclined crack*

We consider a crack inclined with respect to the x_1–x_2 axes defining the prestress directions and the orthotropy axes (see figure 3 in which the shear band should be thought to represent a crack). Therefore, the x_1–x_2 reference system has to be distinguished from the system $\hat{x}_1$–$\hat{x}_2$, where the $\hat{x}_1$-axis is aligned parallel to the crack. The transformation between the two systems is expressed by equation (3.1), while the transformations between incremental displacement, its gradient, nominal stress and constitutive tensor are given by equations (3.2)–(3.4).

The trick to solve the inclined crack problem can be deduced from Savin (1961, see also Sih & Liebowitz 1968) and consists in the introduction of a function analogous to that for an aligned crack (obtained in the electronic supplementary material, see eqns (40), (48), (57) and (63)), but now defined in the $\hat{x}_1$–$\hat{x}_2$ reference system, namely (which automatically satisfies the decaying conditions of fields at infinity)

$$\hat{\psi}^{\circ}_{M}(\hat{x}_1,\hat{x}_2)=\frac{\hat{t}^{\infty}_{2n}}{2\mu}\sum_{j=1}^{2}\mathrm{Re}\left[A^{M}_{j}f(\hat{z}_j)\right], \tag{B 3}$$

where $n{=}1$ and $M{=}\mathrm{II}$ for mode II ($n{=}2$ and $M{=}\mathrm{I}$ for mode I), so that $\hat{t}^{\infty}_{21}$ $\left(\hat{t}^{\infty}_{22}\right)$ is the traction component parallel (orthogonal) to the crack line. Moreover, $f(\hat{z}_j)$ and $\hat{z}_j$ are defined by equations (3.7) and $(3.8)_1$, respectively.

Constants A^{M}_{j} in equation (B 3) can be obtained by imposing the boundary conditions on the crack faces, which are

$$\left.\begin{array}{llll}\hat{t}^{\circ}_{21}(\hat{x}_1,0^{\pm})=0, & \hat{t}^{\circ}_{22}(\hat{x}_1,0^{\pm})=-\hat{t}^{\infty}_{22}, & \forall\ |\hat{x}_1|<l, & \text{for mode I}\\ \hat{t}^{\circ}_{21}(\hat{x}_1,0^{\pm})=-\hat{t}^{\infty}_{21}, & \hat{t}^{\circ}_{22}(\hat{x}_1,0^{\pm})=0, & \forall\ |\hat{x}_1|<l, & \text{for mode II.}\end{array}\right\} \tag{B 4}$$

Imposing the conditions (B 4) yields a linear algebraic system for the real and imaginary parts of constants A^{M}_{j}

$$\begin{bmatrix} c_{11} & c_{21} & c_{12} & c_{22}\\ -c_{21} & c_{11} & -c_{22} & c_{12}\\ c_{31} & c_{41} & c_{32} & c_{42}\\ -c_{41} & c_{31} & -c_{42} & c_{32}\end{bmatrix}\begin{bmatrix}\mathrm{Re}[A^{M}_{1}]\\ \mathrm{Im}[A^{M}_{1}]\\ \mathrm{Re}[A^{M}_{2}]\\ \mathrm{Im}[A^{M}_{2}]\end{bmatrix}=\underbrace{\begin{bmatrix}-1\\0\\0\\0\end{bmatrix}}_{\text{for mode I}}\quad\text{or}\quad\underbrace{\begin{bmatrix}0\\0\\-1\\0\end{bmatrix}}_{\text{for mode II}}, \tag{B 5}$$

where $M{=}\mathrm{I}$ for mode I ($M{=}\mathrm{II}$ for mode II) and coefficients c_{ij} are

$$\left.\begin{aligned}2\mu c_{1j}&=\hat{\mathbb{K}}_{1112}-\hat{\mathbb{K}}_{1222}-\mathrm{Re}\,[W_j][\hat{\mathbb{K}}_{1111}-2\hat{\mathbb{K}}_{1122}-\hat{\mathbb{K}}_{1221}+\hat{\mathbb{K}}_{2222}\\ &\quad+\mathrm{Re}\,[W_j](2\hat{\mathbb{K}}_{1121}-2\hat{\mathbb{K}}_{2122}+\mathrm{Re}\,[W_j]\hat{\mathbb{K}}_{2121})]\\ &\quad+\mathrm{Im}\,[W_j]^2(2\hat{\mathbb{K}}_{1121}-2\hat{\mathbb{K}}_{2122}+3\,\mathrm{Re}\,[W_j]\hat{\mathbb{K}}_{2121}),\\ 2\mu c_{2j}&=\mathrm{Im}\,[W_j][\hat{\mathbb{K}}_{1111}-2\hat{\mathbb{K}}_{1122}-\hat{\mathbb{K}}_{1221}+\hat{\mathbb{K}}_{2222}\\ &\quad+\mathrm{Re}\,[W_j](4\hat{\mathbb{K}}_{1121}-4\hat{\mathbb{K}}_{2122}+3\,\mathrm{Re}\,[W_j]\hat{\mathbb{K}}_{2121})-\mathrm{Im}[W_j]^2\hat{\mathbb{K}}_{2121}],\\ 2\mu c_{3j}&=-\hat{\mathbb{K}}_{1221}+\mathrm{Re}\,[W_j][\hat{\mathbb{K}}_{1121}-\hat{\mathbb{K}}_{2122}+\mathrm{Re}\,[W_j]\hat{\mathbb{K}}_{2121}]-\mathrm{Im}[W_j]^2\hat{\mathbb{K}}_{2121},\\ 2\mu c_{4j}&=\mathrm{Im}[W_j]\left(-\hat{\mathbb{K}}_{1121}+\hat{\mathbb{K}}_{2122}-2\,\mathrm{Re}\,[W_j]\hat{\mathbb{K}}_{2121}\right),\quad j=1,2,\end{aligned}\right\} \tag{B 6}$$

and depend on the crack inclination ϑ_0 and on the prestress and orthotropy parameters ξ, k and η.

The determinant of the coefficient matrix in equation (B 5) is null only when the surface instability condition, equation (A 18), is met, so that in all other cases, system (B 5) can be solved and the solution of the inclined crack follows. Note that when the surface bifurcation condition is approached, the fields, solution of the crack problem, tend to blow up, a peculiarity first noted by Guz (1999 and references quoted therein).

For values of parameters ξ, k and η beyond the surface instability threshold, the obtained solution still works, from a purely mathematical point of view. However, the crack faces cannot be maintained straight after a surface bifurcation point has been passed, so that the solution looses its physical meaning (the incremental energy release rate, obtained in appendix B*c*, becomes negative in this situation).

The perturbed incremental displacement along the crack faces can be obtained in the form

$$\left.\begin{aligned}\hat{v}_1^{\circ M}(\hat{x}_1,\hat{x}_2=0^{\pm}) &= \frac{\hat{t}_{2n}^{\infty}}{2\mu}\,\mathrm{Re}\left[(W_1A_1^M+W_2A_2^M)\left(\hat{x}_1\mp \mathrm{i}\sqrt{l^2-\hat{x}_1^2}\right)\right],\\ \hat{v}_2^{\circ M}(\hat{x}_1,\hat{x}_2=0^{\pm}) &= -\frac{\hat{t}_{2n}^{\infty}}{2\mu}\,\mathrm{Re}\left[(A_1^M+A_2^M)\left(\hat{x}_1\mp \mathrm{i}\sqrt{l^2-\hat{x}_1^2}\right)\right],\end{aligned}\right\} \tag{B 7}$$

so that the jump in incremental displacements across the crack surfaces ($\hat{x}_2=0$, $|\hat{x}_1|<l$) takes the form

$$\left.\begin{aligned}[\![\hat{v}_1^M]\!] &= \frac{\hat{t}_{2n}^{\infty}}{\mu}\,\mathrm{Im}\left[W_1A_1^M+W_2A_2^M\right]\sqrt{l^2-\hat{x}_1^2},\\ [\![\hat{v}_2^M]\!] &= -\frac{\hat{t}_{2n}^{\infty}}{\mu}\,\mathrm{Im}\left[A_1^M+A_2^M\right]\sqrt{l^2-\hat{x}_1^2},\end{aligned}\right\} \tag{B 8}$$

where $n=1$ and $M=\mathrm{II}$ ($n=2$ and $M=\mathrm{I}$) for mode II (mode I).

It is worth noting that the following conditions, proven in the particular cases of null prestress or crack parallel to the orthotropy axes, have been in general verified numerically to hold

$$\mathrm{Re}\left[A_1^{\mathrm{I}}+A_2^{\mathrm{I}}\right]=0,\qquad \mathrm{Re}\left[W_1A_1^{\mathrm{II}}+W_2A_2^{\mathrm{II}}\right]=0, \tag{B 9}$$

showing that the incremental perturbed displacement along the x_1-axis outside the crack is only longitudinal, i.e. $\hat{v}_2^{\circ}=0$ (transversal, i.e. $\hat{v}_1^{\circ}=0$) for mode I (for mode II), a circumstance noted also by Broberg (1999, his §4.14) for infinitesimal anisotropic elasticity.

In addition to equation (B 9), the following conditions are obtained in the particular case of a crack parallel to the orthotropy x_1-axis, $\vartheta_0=0$,

$$\mathrm{Im}\left[W_1A_1^{\mathrm{I}}+W_2A_2^{\mathrm{I}}\right]=0,\qquad \mathrm{Im}\left[A_1^{\mathrm{II}}+A_2^{\mathrm{II}}\right]=0, \tag{B 10}$$

from which the solution obtained in the electronic supplementary material can be easily recovered.

Finally, we note that the incremental stress intensity factors, defined as

$$\dot{K}_{\mathrm{I}} = \lim_{x_1 \to l^+} \frac{\dot{t}_{22}(x_1, x_2 = 0)}{\sqrt{2\pi(x_1 - l)}}, \qquad \dot{K}_{\mathrm{II}} = \lim_{x_1 \to l^+} \frac{\dot{t}_{21}(x_1, x_2 = 0)}{\sqrt{2\pi(x_1 - l)}}, \tag{B 11}$$

follow immediately from the above calculations. These are

$$\dot{K}_{\mathrm{I}} = \dot{t}^{\infty}_{22}\sqrt{\pi l}, \qquad \dot{K}_{\mathrm{II}} = \dot{t}^{\infty}_{21}\sqrt{\pi l}, \tag{B 12}$$

for modes I and II loading, respectively. Note that equations (B 12) coincide with their counterpart in elasticity without prestress, except that now the nominal stress replaces the Cauchy stress.

The inclined crack solution becomes particularly simple in the case when the prestress is null, $k = \eta = 0$. In particular, for mode I we have

$$A^{\mathrm{I}}_j = -(-1)^j \frac{\cos 2\vartheta_0}{2\sqrt{1-\xi}} - \mathrm{i}\frac{1 - \xi - (-1)^j\sqrt{1-\xi}\,\sin 2\vartheta_0}{2(1-\xi)\sqrt{\xi}}, \quad j = 1, 2, \tag{B 13}$$

while for mode II we have

$$A^{\mathrm{II}}_j = (-1)^j \left[\frac{\sin 2\vartheta_0}{2\sqrt{1-\xi}} + \mathrm{i}\frac{\cos 2\vartheta_0}{2\sqrt{(1-\xi)\xi}}\right], \quad j = 1, 2. \tag{B 14}$$

The following properties can also be proven:

$$W_1 A^{\mathrm{I}}_1 + W_2 A^{\mathrm{I}}_2 = 0, \qquad A^{\mathrm{II}}_1 + A^{\mathrm{II}}_2 = 0. \tag{B 15}$$

An interesting feature that does not hold when the prestress is present and the crack is inclined can be deduced from equations (B 8), (B 15)$_1$ and (B 14), namely that a mode I (mode II) loading does not produce longitudinal, v_1 (transversal, v_2), incremental displacements along the crack line, so that for $\hat{x}_2 = 0$ and $|\hat{x}_1| < l$, we have

$$[\![\hat{\boldsymbol{v}}]\!] = \left\{\frac{\hat{t}^{\infty}_{21}}{\mu\sqrt{\xi}}\sqrt{l^2 - \hat{x}_1^2}, \quad \frac{\hat{t}^{\infty}_{22}}{\mu\sqrt{\xi}}\sqrt{l^2 - \hat{x}_1^2}\right\}, \tag{B 16}$$

which is independent of the crack inclination ϑ_0.

(*b*) *Shear bands interacting with a finite-length crack*

In the spirit of the perturbative approach proposed by Bigoni & Capuani (2002, 2005), the role of shear banding in the incremental deformation fields around a crack of length $2l$ is investigated. The crack is considered in a J_2-deformation theory material near the EC/H boundary, aligned parallel to the principal stress axis x_1 (lying therefore in a symmetry axis with respect to the conjugate band directions), and loaded under incremental mode I. In particular, for the value of hardening exponent $N = 0.8$, the critical logarithmic strain for localization (and the shear band inclination with respect to the x_1-axis) is $\varepsilon \approx 1.032$ ($\vartheta_0 \approx 19.60°$).

The level sets of the modulus of incremental deviatoric strain have been mapped in figure 6 with a choice of η, namely $\eta/k = 0.775$, such that the Hill exclusion condition (A 2) is satisfied.

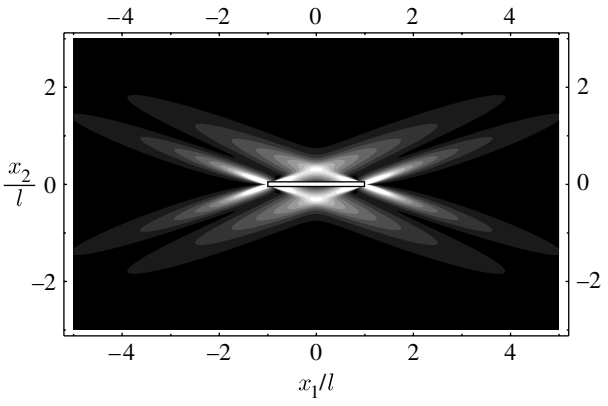

Figure 6. Level sets of the modulus of incremental deviatoric strain evidencing interaction of shear bands and mechanical fields near a crack of length $2l$ under mode I incremental loading. A J_2-deformation theory material has been considered at high-strain hardening $N=0.8$, prestrained near the elliptic border $\varepsilon=0.981$. The crack is horizontal, while the shear bands are inclined at $\pm 19.60°$. Note that four shear bands emerge.

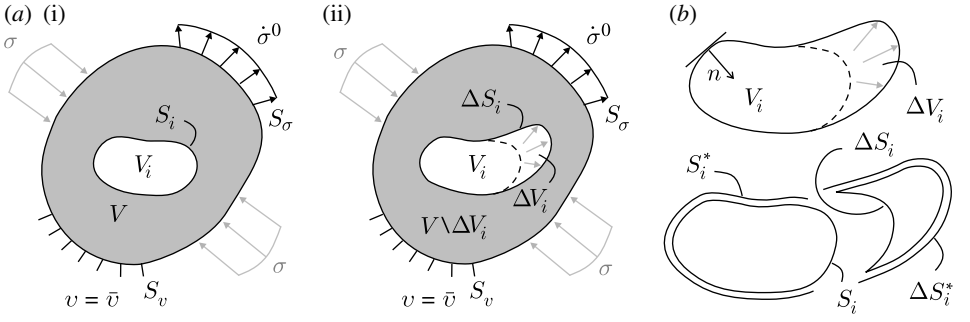

Figure 7. (*a*(i),(ii)) Two elastic prestressed bodies are compared, having identical shape, boundary conditions, elastic properties, prestress and prestrain, but voids of different size. (*b*) The detail of the void and its surface is reported; note the unit normal vector, defined to point outward from the elastic body and towards the void. Incremental deformation of prestressed solids are considered, so that the surface of the void can be subjected to finite dead loading and surface $\mathbf{\Delta} S_i^*$ must be subjected to the nominal tractions present on the same surface embedded in the material in the configuration in (*a*(i)).

Results are qualitatively analogous for different values of strain hardening and for mode II loading; in particular, the mode II incremental deformation fields are dominated near the elliptic border by localized deformations aligned parallel to the two shear band conjugate directions, in a way quite similar to figure 6.

We can observe that *two symmetric shear bands emerge near the crack tip,* and their interaction may lead to failure of the material under shear in front of the crack, a situation compatible with mode I growth, to be interpreted as a sort of 'alternating sliding off and cracking', as suggested by McClintock (1971) and Kardomateas & McClintock (1989). The situation is more complicated for mode II loading, but our results agree with the consideration made by Hallbäck & Nilsson (1994) that 'mode II failure results when the direction of the prospective shear band coincides with the crack surface direction, while mode I-type failure occurs when the shear bands are inclined to the direction of crack surfaces'.

(c) *Incremental energy release rate for crack growth*

We slightly generalize Rice (1968) and start referring to figure 7 and comparing two incremental boundary-value problems (for finite bodies subjected to identical conditions on the external boundaries $S_\sigma \cup S_v$, namely prescribed incremental nominal tractions $\dot{\boldsymbol{\sigma}}^0$ on S_σ and incremental displacements $\boldsymbol{v} = \bar{\boldsymbol{v}}$ on S_v) differing only in the sizes of the void that they contain. Note that we are addressing an incremental problem, so that the surface of the void can be loaded by dead loading.

In particular, the void in the body on figure 7*a*(ii) (of volume $V_i \cup \Delta V_i$, enclosed by surface $S_i^* \cup \Delta S_i^*$) has been obtained by increasing the size of the void in the body on figure 7*a*(i) (of volume V_i, enclosed by surface S_i).

Since we want to include prestress in an incremental formulation, nominal (finite) dead tractions identical to those existing within the material containing the void V_i must be applied on the surface ΔS_i^* of the material containing the void $V_i \cup \Delta V_i$.

We define the incremental displacement and nominal traction fields, solutions to the two problems, as $\boldsymbol{v}^0$ and $\dot{\boldsymbol{t}}^0$ for the problem in figure 7*a*(i) and $\boldsymbol{v} = \boldsymbol{v}^0 + \tilde{\boldsymbol{v}}$ and $\dot{\boldsymbol{t}} = \dot{\boldsymbol{t}}^0 + \tilde{\boldsymbol{t}}$ for the problem in figure 7*a*(ii). Since the void surfaces are subjected to dead loading, $\dot{\boldsymbol{t}}^{0T}\boldsymbol{n} = \boldsymbol{0}$ and $\dot{\boldsymbol{t}}^{T}\boldsymbol{n} = \boldsymbol{0}$, within V_i and $V_i \cup \Delta V_i$, respectively.

The two bodies are assumed to be identically prestressed and prestrained, although not necessarily in a homogeneous way. If the expedient of prescribing 'ad hoc' dead tractions on ΔS_i^* is not considered and the void surface is free of tractions, in order to have identical prestress and prestrain, the two current configurations shown in figure 7 must have special geometries and loadings, as will be the case of a crack aligned parallel to a principal stress direction with the other principal stress to be null and, more important, of our shear band model (§3).

The incremental potential energy decrease for a void growth in an elastic (incompressible or compressible, generically anisotropic and prestressed) body takes an expression analogous to that reported by Rice (1968, p. 207, his eqn (55)), namely

$$-\Delta\dot{P} = \int_{\Delta V_i} \phi(\nabla \boldsymbol{v}^0)\, \mathrm{d}V - \frac{1}{2}\int_{\Delta S_i^*} \boldsymbol{n}\cdot\boldsymbol{t}^0\tilde{\boldsymbol{v}}\, \mathrm{d}S, \tag{B 17}$$

a quantity which when positive implies void *growth*. Note that the scalar function ϕ is the incremental gradient potential defined as

$$\dot{t}_{ij} = \frac{\partial\phi(\nabla\boldsymbol{v})}{\partial v_{j,i}} + \dot{p}\,\delta_{ij}, \qquad \phi(\nabla\boldsymbol{v}) = \frac{1}{2}\, v_{j,i}\mathbb{K}_{ijhk}v_{k,h}. \tag{B 18}$$

Turning now the attention to a thin void inclusion, namely a crack aligned parallel to the $\hat{x}_1$-axis (figure 3), the volume integral in equation (B 17) vanishes, so that taking the limit of the length increase $\Delta l \to 0$ at fixed incremental stress intensity factor $\dot{K}$, equation (B 17) becomes

$$\dot{G} = -\frac{\mathrm{d}\dot{P}}{\mathrm{d}l} = \lim_{\Delta l\to 0}\frac{1}{2\Delta l}\int_0^{\Delta l} \hat{t}_{2i}(r,0)[\![\hat{v}_i(\Delta l - r,\pi)]\!]\, \mathrm{d}r, \tag{B 19}$$

where the symbol $\hat{}$ denotes that we are using the inclined crack solution, the repeated index is summed; r denotes the radial distance from the crack tip and 0 and π indicate values of the polar coordinate (anticlockwise) angle singling out r from the $\hat{x}_1$-axis (so that $\theta = 0$ corresponds to points ahead of the crack tip).

Equation (B 19) defines *the incremental energy release rate for a mixed-mode growth of a crack in an elastic incompressible or compressible body, generically anisotropic and prestressed.*

The proof that the incremental energy release rate coincides with the path-independent incremental $\dot{J}$-integral

$$\dot{J} = \int_{\Gamma} \left(\hat{\phi} \hat{n}_1 - \hat{n}_j \hat{t}_{ji} \frac{\partial \hat{v}_i}{\partial \hat{x}_1} \right) \mathrm{d}\Gamma \tag{B 20}$$

has not yet been explicitly obtained, but the validity of $\dot{G} = \dot{J}$ has been verified numerically.

The incremental energy release rate (B 19) can be developed making use of the asymptotic near-tip incremental nominal stress ahead of the crack

$$\hat{t}_{22}(r,0) = \frac{\dot{K}_{\mathrm{I}}}{\sqrt{2\pi r}}, \qquad \hat{t}_{21}(r,0) = \frac{\dot{K}_{\mathrm{II}}}{\sqrt{2\pi r}}, \tag{B 21}$$

and incremental displacement on the crack faces (where constants have been neglected)

$$\left.\begin{aligned} \hat{v}_1(\Delta l - r, \pm\pi) &= \pm \frac{\sqrt{2l}\sqrt{\Delta l - r}}{2\mu} \mathrm{Im}\left[\hat{t}^{\infty}_{22}(W_1 A^{\mathrm{I}}_1 + W_2 A^{\mathrm{I}}_2) + \hat{t}^{\infty}_{21}(W_1 A^{\mathrm{II}}_1 + W_2 A^{\mathrm{II}}_2) \right], \\ \hat{v}_2(\Delta l - r, \pm\pi) &= \mp \frac{\sqrt{2l}\sqrt{\Delta l - r}}{2\mu} \mathrm{Im}\left[\hat{t}^{\infty}_{22}(A^{\mathrm{I}}_1 + A^{\mathrm{I}}_2) + \hat{t}^{\infty}_{21}(A^{\mathrm{II}}_1 + A^{\mathrm{II}}_2) \right], \end{aligned}\right\} \tag{B 22}$$

holding for 'small' Δl.

Employing the asymptotic near-tip representations (B 21) and (B 22) in equation (B 19), we obtain

$$\begin{aligned} \dot{G} = -\dot{K}^2_{\mathrm{I}} \frac{\mathrm{Im}\left[A^{\mathrm{I}}_1 + A^{\mathrm{I}}_2 \right]}{4\mu} + \dot{K}^2_{\mathrm{II}} \frac{\mathrm{Im}\left[W_1 A^{\mathrm{II}}_1 + W_2 A^{\mathrm{II}}_2 \right]}{4\mu} \\ + \dot{K}_{\mathrm{I}} \dot{K}_{\mathrm{II}} \frac{\mathrm{Im}\left[W_1 A^{\mathrm{I}}_1 + W_2 A^{\mathrm{I}}_2 - A^{\mathrm{II}}_1 - A^{\mathrm{II}}_2 \right]}{4\mu}, \end{aligned} \tag{B 23}$$

representing the incremental energy release rate for an inclined crack loaded in mixed mode in a prestressed, orthotropic and incompressible material.

From equation (B 23) *the incremental energy release rate for a mixed-mode loading of a crack parallel to the orthotropy axes* (i.e. $\vartheta_0 = 0$) can be made explicit

$$\dot{G} = \frac{\Lambda}{\mu} \frac{\dot{K}^2_{\mathrm{I}} \sqrt{1-k} + \dot{K}^2_{\mathrm{II}} \sqrt{1+k}}{(2\xi - \eta + \Lambda)^2 \sqrt{2\xi - 1 - \Lambda} - (2\xi - \eta - \Lambda)^2 \sqrt{2\xi - 1 + \Lambda}}, \tag{B 24}$$

where there is no coupling between the two modes I and II.

Another interesting special case is that of null prestress, in which for an inclined crack the following expression of the incremental energy release rate can be obtained:

$$\dot{G} = \frac{\dot{K}^2_{\mathrm{I}} + \dot{K}^2_{\mathrm{II}}}{4\mu\sqrt{\xi}}, \tag{B 25}$$

which agrees with the known isotropic elasticity solution in the incompressible limit, recovered for $\xi = 1$.

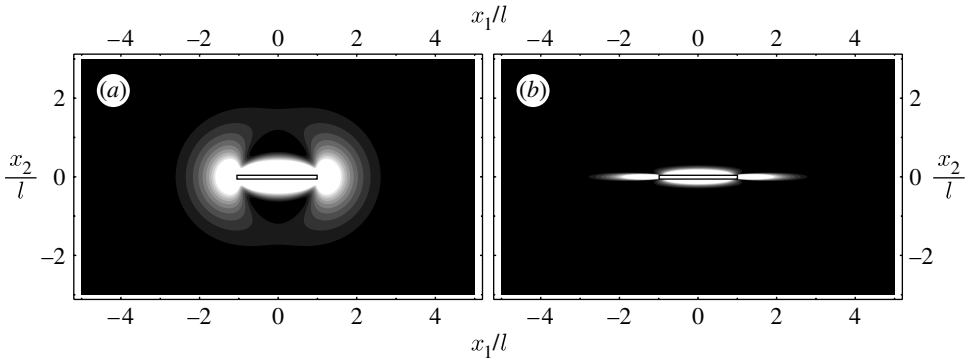

Figure 8. Level sets of the modulus of incremental deviatoric strain, near a shear band of length $2l$ ($\vartheta_0=0°$) in an incrementally isotropic, $\xi=1$, material (*a*) without prestress, $k=0$, and (*b*) prestressed near, $k=\eta=0.95$, the EI/P boundary. Mode II incremental loading is considered.

Appendix C. Further results on the stress state near a shear band

More results on the predicted incremental strain state near a shear band loaded under incremental Mode II in ductile materials are provided here in the case of a material approaching the parabolic boundary and of a J_2-deformation theory material at low- and high-strain hardening $N=0.1$ and 0.8, respectively.

(*a*) *Shear band at the EI/P boundary*

All points of the EI/P boundary can be approached while the Hill exclusion condition holds true when $\eta=k>0$, corresponding to a uniaxial tensile stress state, $\sigma_1>0$, $\sigma_2=0$. In this situation, one shear band forms at the EI/P boundary, $k=1$, parallel to the tensile loading direction (A 17) so that the problem is symmetric and the aligned crack solution (obtained in the electronic supplementary material, eqn (57)), can be used. In fact, due to symmetry, the normal displacement increment and all nominal incremental traction components are null (and therefore a fortiori continuous) at the shear band boundary, under a mode II loading increment.

The shear band solution has been used to obtain results shown in figure 8, where the level sets of incremental deviatoric strain are reported at different levels of prestress, namely at null prestress, $k=0$, and at $k=0.95$, a value very close to the EI/P boundary. Results similar to those obtained in figure 8, but limited to fields near the tip of the shear band can also be obtained employing the asymptotic analysis presented by Radi *et al.* (2002).

It should be noted from figure 8 that the incremental deformation field evidences a strong focusing in the direction of the shear band. Moreover, the incremental energy release rate for shear band growth can be deduced from the formula for crack advance under mode II, equation (B 24). The energy released for an incremental advance of shear band has the typical behaviour shown in figure 5, showing an asymptote at the EI/P boundary.

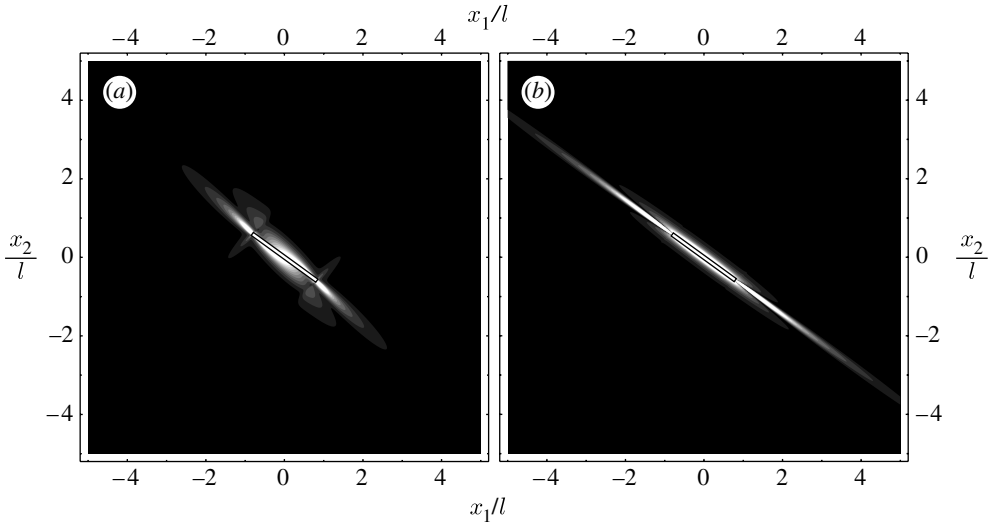

Figure 9. Level sets of the modulus of incremental deviatoric strain, near a shear band of length $2l$ ($\vartheta_0 = 35.95°$) in a J_2-deformation theory material at low ($N=0.1$)-strain hardening, (*a*) not prestrained ($\varepsilon=0$) and (*b*) near the EC/H boundary ($\varepsilon=0.306$). Mode II incremental loading is considered.

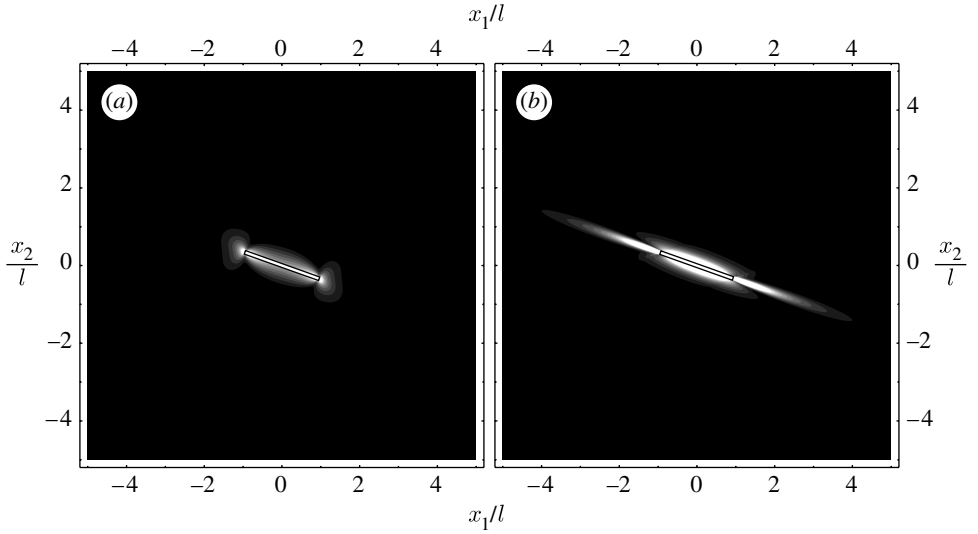

Figure 10. Level sets of the modulus of incremental deviatoric strain, near a shear band of length $2l$ ($\vartheta_0 = 19.60°$) in a J_2-deformation theory material at high ($N=0.8$)-strain hardening, (*a*) not prestrained ($\varepsilon=0$) and (*b*) near the EC/H boundary ($\varepsilon=0.981$). Mode II incremental loading is considered.

(*b*) *Shear band at the EC/H boundary*

Level sets of the modulus of incremental deviatoric strain for a J_2-deformation theory material (which is a particular case of the developed theory) are reported in figure 9 for low ($N=0.1$) and in figure 10 for high ($N=0.8$) strain hardening.

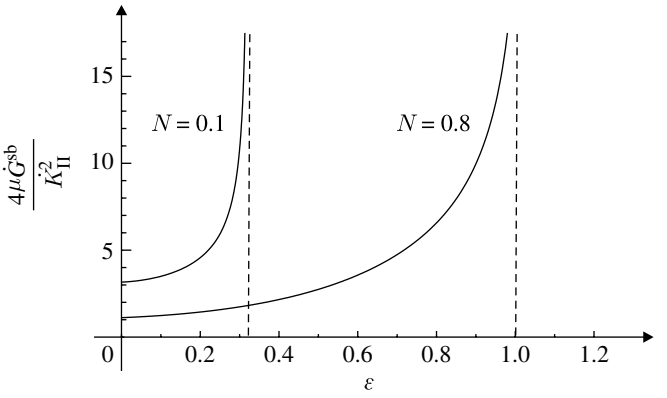

Figure 11. Incremental energy release rate for shear band growth in a J_2-deformation theory material at low ($N=0.1$)- and high ($N=0.8$)-strain hardening, as a function of the prestrain ε. The curve presents an asymptote at the EI/P boundary ($\varepsilon \approx 0.322$ for $N=0.1$ and $\varepsilon \approx 1.032$ for $N=0.8$), so that shear band growth becomes 'unrestrainable' when prestress approaches this point.

In both cases, null prestrain (and prestress) and a value of prestrain near the EC/H boundary have been considered. Moreover, parameter η has been taken equal to $0.311k$ for $N=0.1$ and $0.775k$ for $N=0.8$, to ensure the validity of the Hill exclusion condition (A 2) near the EC/H boundary. Note that, for null prestrain $\varepsilon=0$, the shear band model behaves as a fracture, since the normal component of incremental displacement remains continuous for a crack in an orthotropic incompressible material at null prestress. Therefore, figures 9*a* and 10*a* are identical to the analogue cases reported for the inclined crack in the electronic supplementary material (figs 4*b* and 5*b*). The difference between the shear band model and the crack becomes evident while comparing figs 4*d* and 5*d* of the electronic supplementary material with figures 9*b* and 10*b*, where in the former figures both conjugate directions of shear bands are activated under mode II loading, while only the direction aligned to the shear band is activated in the latter case.

Calculations of the incremental energy release rate for an infinitesimal shear band advance $\dot{G}^{sb}$ (made dimensionless by multiplication by $4\mu/\dot{K}_{II}^2$) for shear band growth in a J_2-deformation theory material at low ($N=0.1$) and high ($N=0.8$) strain hardening are reported in figure 11.

References

Aifantis, E. C. 1987 The physics of plastic deformation. *Int. J. Plast.* **3**, 211–247. (doi:10.1016/0749-6419(87)90021-0)

Aifantis, K. E. & Willis, J. R. 2005 The role of interfaces in enhancing the yield strength of composites and polycrystals. *J. Mech. Phys. Solids* **53**, 1047–1070. (doi:10.1016/j.jmps.2004.12.003)

Bei, H., Xie, S. & George, E. P. 2006 Softening caused by profuse shear banding in a bulk metallic glass. *Phys. Rev. Lett.* **96**, 105 503. (doi:10.1103/PhysRevLett.96.105503)

Benallal, A. & Bigoni, D. 2004 Effects of temperature and thermo-mechanical couplings on material instabilities and strain localization of inelastic materials. *J. Mech. Phys. Solids* **52**, 725–753. (doi:10.1016/S0022-5096(03)00118-2)

Bigoni, D. & Capuani, D. 2002 Green's function for incremental nonlinear elasticity: shear bands and boundary integral formulation. *J. Mech. Phys. Solids* **50**, 471–500. (doi:10.1016/S0022-5096(01)00090-4)

Bigoni, D. & Capuani, D. 2005 Time-harmonic Green's function and boundary integral formulation for incremental nonlinear elasticity: dynamics of wave patterns and shear bands. *J. Mech. Phys. Solids* **53**, 1163–1187. (doi:10.1016/j.jmps.2004.11.007)

Bigoni, D. & Loret, B. 1999 Effects of elastic anisotropy on strain localization and flutter instability in plastic solids. *J. Mech. Phys. Solids* **47**, 1409–1436. (doi:10.1016/S0022-5096(98)00119-7)

Biot, M. A. 1965 *Mechanics of incremental deformations*. New York, NY: Wiley.

Broberg, K. B. 1999 *Cracks and fracture*. San Diego, CA: Academic Press.

Cottrell, A. H. 1953 *Dislocations and plastic flow in crystals*. Oxford, UK: Clarendon Press.

Cristescu, N. D., Craciun, E. M. & Soós, E. 2004 *Mechanics of elastic composites*. Boca Raton, FL: Chapman & Hall; CRC.

Dal Corso, F., Bigoni, D. & Gei, M. 2008 The stress concentration near a rigid line inclusion in a prestressed, elastic material. Part I. Full-field solution and asymptotics. *J. Mech. Phys.* **56**, 815–838. (doi:10.1016/j.jmps.2007.07.002)

Fenistein, D. & van Hecke, M. 2003 Kinematics—wide shear zones in granular bulk flow. *Nature* **425**, 256. (doi:10.1038/425256a)

Gajo, A., Bigoni, D. & Muir Wood, D. 2004 Multiple shear band development and related instabilities in granular materials. *J. Mech. Phys. Solids* **52**, 2683–2724. (doi:10.1016/j.jmps.2004.05.010)

Gioia, G. & Ortiz, M. 1996 The two-dimensional structure of dynamic boundary layers and shear bands in thermoviscoplastic solids. *J. Mech. Phys. Solids* **44**, 251–292. (doi:10.1016/0022-5096(95)00071-2)

Guduru, P. R., Ravichandran, G. & Rosakis, A. J. 2001 Observations of transient high temperature vortical microstructures in solids during adiabatic shear banding. *Phys. Rev. E* **64**, 036 128. (doi:10.1103/PhysRevE.64.036128)

Guz, A. N. 1999 *Fundamentals of the three-dimensional theory of stability of deformable bodies*. Berlin, Germany: Springer.

Hallbäck, N. & Nilsson, F. 1994 Mixed-mode I/II fracture behaviour of an aluminium alloy. *J. Mech. Phys. Solids* **42**, 1345–1374. (doi:10.1016/0022-5096(94)90001-9)

Hill, R. 1958 A general theory of uniqueness and stability in elastic-plastic solids. *J. Mech. Phys. Solids* **6**, 236–249. (doi:10.1016/0022-5096(58)90029-2)

Hill, R. & Hutchinson, J. W. 1975 Bifurcation phenomena in the plane tension test. *J. Mech. Phys. Solids* **23**, 239–264. (doi:10.1016/0022-5096(75)90027-7)

Hutchinson, J. W. & Neale, K. W. 1979 Finite strain J_2-deformation theory. In *Proc. IUTAM Symp. on Finite Elasticity* (eds D. E. Carlson and R. T. Shield), pp. 237–247. The Hague, The Netherlands: Martinus Nijhoff.

Hutchinson, J. W. & Tvergaard, V. 1981 Shear band formation in plane strain. *Int. J. Solids Structures* **17**, 451–470. (doi:10.1016/0020-7683(81)90053-6)

Kardomateas, G. A. & McClintock, F. A. 1989 Shear band characterization of mixed mode I and II fully plastic crack growth. *Int. J. Fracture* **40**, 1–12. (doi:10.1007/BF01150863)

Korbel, A. & Bochniak, W. 2004 Refinement and control of the metal structure elements by plastic deformation. *Scripta Mater.* **51**, 755–759. (doi:10.1016/j.scriptamat.2004.06.020)

Lekhnitskii, S. G. 1981 *Theory of elasticity of an anisotropic body*. Moscow, Russia: Mir Publisher.

Lewandowski, J. J. & Greer, A. L. 2006 Temperature rise at shear bands in metallic glasses. *Nat. Mater.* **5**, 15–18. (doi:10.1038/nmat1536)

McClintock, F. A. 1971 Plasticity aspects of fracture. In *Fracture. An advanced treatise*, vol. III (ed. H. Liebowitz), pp. 47–225. New York, NY: Academic Press Inc.

Needleman, A. & Ortiz, M. 1991 Effects of boundaries and interfaces on shear-band localization. *Int. J. Solids Structures* **28**, 859–877. (doi:10.1016/0020-7683(91)90005-Z)

Needleman, A. & Tvergaard, V. 1983 *Finite elements: special problems in solid mechanics*, vol. V (eds J. T. Oden & G. F. Carey), p. 94.

Palmer, A. C. & Rice, J. R. 1973 The growth of slip surfaces in the progressive failure of over-consolidated clay. *Proc. R. Soc. A* **332**, 527–548. (doi:10.1098/rspa.1973.0040)

Petryk, H. 1997 Plastic instability: criteria and computational approaches. *Arch. Comput. Meth. Eng.* **4**, 111–151.

Petryk, H. & Thermann, K. 2002 Post-critical plastic deformation in incrementally nonlinear materials. *J. Mech. Phys. Solids* **50**, 925–954. (doi:10.1016/S0022-5096(01)00131-4)

Piccolroaz, A., Bigoni, D. & Willis, J. R. 2006 A dynamical interpretation of flutter instability in a continuous medium. *J. Mech. Phys. Solids* **54**, 2391–2417. (doi:10.1016/j.jmps.2006.05.005)

Puzrin, A. M. & Germanovich, L. N. 2005 The growth of shear bands in the catastrophic failure of soils. *Proc. R. Soc. A* **461**, 1199–1228. (doi:10.1098/rspa.2004.1378)

Radi, E., Bigoni, D. & Capuani, D. 2002 Effects of prestress on crack-tip fields in elastic, incompressible solids. *Int. J. Solids Structures* **39**, 3971–3996. (doi:10.1016/S0020-7683(02)00252-4)

Rice, J. R. 1968 Mathematical analysis in the mechanics of fracture. In *Fracture. An advanced treatise*, vol. II (ed. H. Liebowitz), pp. 191–311. New York, NY: Academic Press Inc.

Rice, J. R. 1973 In *Plasticity and soil mechanics* (ed. A. C. Palmer), p. 263. Cambridge, UK: Cambridge University Engineering Department.

Rittel, D., Wang, Z. G. & Merzer, M. 2006 Adiabatic shear failure and dynamic stored energy of cold work. *Phys. Rev. Lett.* **96**, 075 502. (doi:10.1103/PhysRevLett.96.075502)

Rudnicki, J. W. & Rice, J. R. 1975 Conditions for the localization of deformation in pressure-sensitive dilatant materials. *J. Mech. Phys. Solids* **23**, 371–394. (doi:10.1016/0022-5096(75)90001-0)

Savin, G. N. 1961 *Stress concentration around holes*. Oxford, UK: Pergamon Press.

Sih, G. C. & Liebowitz, H. 1968 In *Fracture. An advanced treatise*, vol. II (ed. H. Liebowitz), p. 67. New York, NY: Academic Press Inc.

Sulem, J. & Ouffroukh, H. 2006 Hydromechanical behaviour of Fontainebleau sandstone. *Rock Mech. Rock Eng.* **39**, 185–213. (doi:10.1007/s00603-005-0065-4)

Tvergaard, V. 1982 Influence of void nucleation on ductile shear fracture at a free surface. *J. Mech. Phys. Solids* **30**, 399–425. (doi:10.1016/0022-5096(82)90025-4)

Xue, Q. & Gray, G. T. 2006 Development of adiabatic shear bands in annealed 316L stainless steel: Part I. Correlation between evolving microstructure and mechanical behavior. *Metall. Mater. Trans. A* **37**, 2435–2446. (doi:10.1007/BF02586217)